Proceedings of the Thirtieth (2020) International Ocean and Polar Engineering Conference **www.isope.org**
Shanghai, China, October 11-16, 2020

ISBN 978-1-880653-84-5; ISSN 1098-6189

Experimental Study on Vortex-Induced Motions of Floating Circular Single Cylinders with Low Aspect Ratio and Different Heave Plate Geometries

Rodolfo Trentin Gonçalves[1]
Raíza Oliveira Pereira da Silva[2]
Matheus Antonio Marques[3]
Shinichiro Hirabayashi[4]
Gustavo Roque da Silva Assi[2]
Alexandre Nicolaos Simos[2]
Hideyuki Suzuki[1]

[1]OSPL - Ocean Space Planning Laboratory, Dept. of Systems Innovation, School of Engineering, The University of Tokyo
Bunkyo-ku, Tokyo, Japan

[2]Dept. of Naval Architecture and Ocean Engineering, Escola Politécnica, University of São Paulo
São Paulo, SP, Brazil

[3]Dept. of Mechanical Engineering, Federal University of Pernambuco
Recife, PE, Brazil

[4]OSPL - Ocean Space Planning Laboratory, Dept. of Ocean Technology, Policy, and Environment, School of Frontier Sciences, The University of Tokyo
Kashiwa-shi, Chiba, Japan

ABSTRACT

Experiments regarding vortex-induced motions (VIM) of floating circular cylinders with low aspect ratio, $L/D = 2.0$, and different heave plate configurations were carried out in a recirculation water channel; where D is the diameter and L is the submerged length of the cylinder. The floating circular cylinders were elastically supported by a set of linear springs to provide low structural damping on the system. Twelve different heave plate conditions were tested combining three heave plate diameters, D_p, and four heave plate heights, H_p. The geometry conditions were $D_p/D = 1.2$, 1.6 and 2.0, and H_p/D=0.0, 0.2, 0.4, and 0.6. Additionally, a single-cylinder case without a heave plate was experimented, i.e., $D_p/D = 1.0$. These different heave plate conditions were selected to promote changes in the structures shedding around the free end of the cylinder. The aim was to understand the heave plate effects on the VIM amplitudes. The range of Reynolds number covered $3{,}000 < Re < 24{,}000$, and the reduced velocity ranged $2 < V_r < 15$. The increase in the heave plate dimensions decreased the VIM amplitudes. The increase in the heave plate height decreased the drag force. The heave plate may be a reasonable solution to mitigate the VIM of offshore single column systems and perhaps of multi-column floaters.

KEYWORDS: vortex-induced motions, floating model, circular cylinder, heave plate, model tests.

NOMENCLATURE

A_x	nominal amplitude for the motions in the in-line direction
A_y	nominal amplitude for the motions in the transverse direction
C_a	additional mass coefficient
C_D	drag coefficient
D	diameter of the cylinder subjected to vortex shedding
D_p	diameter of heave plate
f_0	natural frequency of the transverse motion in still water
f_{0x}	natural frequency of the motion in the in-line direction in still water
f_{0y}	natural frequency of the motion in the transverse direction in still water
$\overline{FH_x}$	mean of the hydrodynamic force in the in-line direction
h	distance of cylinder free end to the bottom of the channel
L	column height above the heave plate to the free surface
H	height of the channel
H_p	height of the heave plate
k	spring stiffness parameter
KG	distance from keel to center of gravity

L_q	length of the rectangular support
m_a	additional mass
m	total mass of the model
T_{0y}	natural period in still water
T_{0y}	natural period of the transverse motion in still water
T_{0x}	natural period of the in-line motion in still water
S	column area exposed to the current
U	incident current velocity
V_r	reduced velocity
W_q	width of the rectangular support
x	x-axis of the coordinate system inthe free- surface section
y	y-axis of the coordinate system inthe free- surface section
ρ	water density
ζ_s	structural damping
ζ_w	hydrodynamic damping coefficient in still water

INTRODUCTION

The vortex-induced motions (VIM) is an issue that concerns the offshore industry. Since the new projects reach large dimensions of single and multi-column systems, these systems are exposed to the ocean environment as current incidence, and they are subject to VIM amplitudes. New floating offshore wind turbines (FOWTs) have demanded dimension changes to meet the turbine limits of working time as the acceleration of the nacelle of the rotor and inclination angles of the tower. Different FOWT platform configurations have been studied, as can be seen in Liu *et al.* (2016), Lemmer *et al.* (2018), Suzuki *et al.* (2019), and Mello *et al.* (2019). However, few works addressing the VIM phenomenon could be found in the literature; the ones encountered were reported by Carlson & Sadeghi (2017) and Gonçalves *et al.* (2019) for a single and a multi-column FOWT, respectively.

A usual solution for minimizing the vertical response in waves of FOWT was the introduction of the heave plates. The heave plate is a plate attached to the column bottom aiming to increase the added mass and damping of the system and, consequently, decreasing the vertical response in waves of the FOWT. The benchmarking FOWT semi-submersible type (OC4 phase II) presents this device to improve the hydrodynamic behavior, as can be seen in Robertson *et al.* (2014).

For the single column platforms, studies regarding the heave plate structure focused on the hydrodynamic effect, especially on heave motion reduction. For example, numerical analyses were performed in Thiagarajan *et al*. (2002) and Tao & Cai (2004) to optimize the heave plate geometry. An experimental example of the investigation of heave plate hydrodynamic characteristics can be seen in Li *et al.* (2013).Both works confirmed that the heave plate structures could be used to reduce heave motions, and they can also be applied to multi-column systems.

The increase of the heave plate height can cause an additional drag due to the current and wave incidences; thus, the geometry of the heave plate must be carefully understood. For example, the works by Moreno *et al.* (2015), Pavon & Iglesias (2015), Barrio *et al.* (2019), and Mello *et al.* (2019) presented a comparison of experimental and numerical analyses for different heave plate configurations to find the best geometry to reduce the hydrodynamics in waves with low increase of the drag forces.

In Mello *et al.* (2019), an analysis of the use of heave plates with height to improve the FOWT performance in waves was presented. The work was developed for designing a FOWT to operate in Brazilian waters. The multi-column system presented four vertical columns. Heave plates were positioned at the bottom of each column, and the use of heave plate height was analyzed to help to tune the natural periods in heave, roll, and pitch, without further increasing the diameter of the plates. A combination of three heave plate diameter, D_p, and three heave plate heights, H_p, were studied. Decay tests for heave, pitch, and surge were performed to evaluate the added mass and damping levels. Further, regular and irregular wave tests were performed to validate a numerical model using the potential theory.

Following the same geometry parameters investigated by Mello *et al.* (2019), the present work aims to investigate the effect of the heave plate geometry subject to the incidence current and, consequently, the VIM amplitudes on a single floating cylinder/column. Results regarding VIM amplitudes in the in-line and directions are presented for each configuration, as well as the drag force coefficient.

EXPERIMENTAL SETUP

All the experiments were carried out in a recirculating water channel at the Fluid & Dynamics Research Group Laboratory (NDF), facility of the University of São Paulo (USP), Brazil. The dimension of the test section is 7,500x700x700mm, and the flow has low levels of turbulence (less than 2%). The pump system can operate properly with free-stream velocities up to 0.40m/s. Further details concerning the water channel can be found in Assi *et al*. (2006).

The floating cylinder was elastically supported by a set of four springs with the same stiffness parameter, $k = 0.73$N/m, distributed in 0º, 90º, 180º, and 270º; The springs were fixed on a rectangular support with $L_q = 1{,}090$mm in length and $W_q = 610$mm in width, respectively; as can be seen in Fig 1. The mooring configuration provided a resultant stiffness coefficient in the in-line and transverse directions of $k_x = 2.49\text{N/m}$ and $k_y = 2.31\text{N/m}$. The water height of the channel was kept constant during the tests, $H = 536$mm. The distance between the cylinder free end and the bottom of the channel was $h = 286$mm.

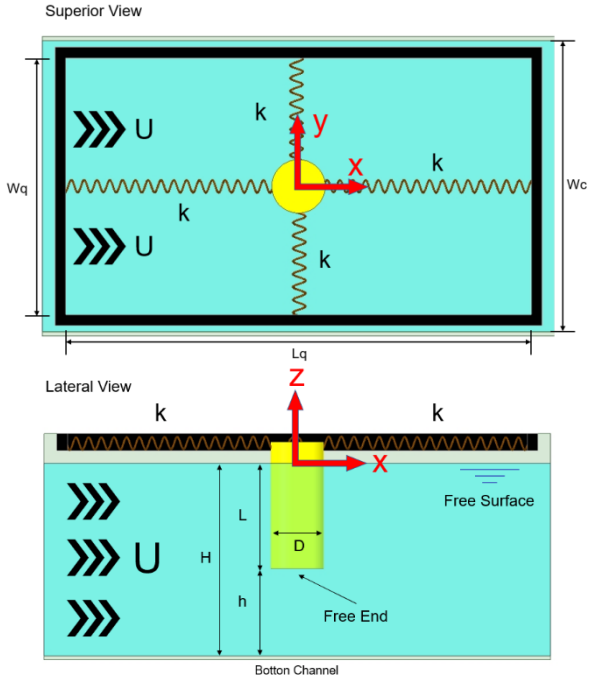

Fig 1. Experimental setup and dimensional parameters of the water channel and model.

The cylinder was free to move in the 6dof.The motions were measured using an optical motion capture system, Qualisys®. A view of the experimental apparatus can be seen in Fig 2.

The models were made of Polyvinyl Chloride (PVC) with diameter $D = 125$mmwith low aspect ratio, $L/D = 2.0$, where L is the submerged length of the cylinder. Twelve different heave plate conditions were tested combining three heave plate diameters, D_p, and four heave plate heights, H_p. The geometry conditions were $D_p/D = 1.2$, 1.6 and 2.0, and H_p/D=0.0, 0.2, 0.4, and 0.6. Additionally, a single-cylinder case without a heave plate was experimented, i.e., $D_p/D = 1.0$. Different views and all configurations of the cylinders experimented can be seen in Fig 3 to Fig 5.

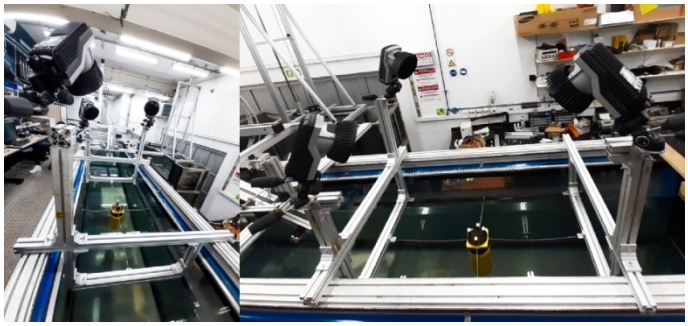

Fig 2. Experimental arrangement of the optical motion capture system and the floating cylinder elastically supported by a set of four springs.

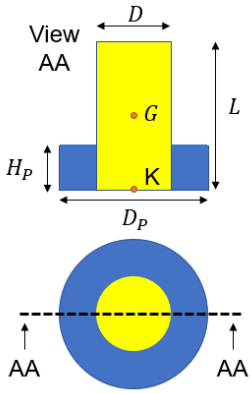

Fig 3. Main dimension parameters of the cylinders.

The natural frequencies in still water in both directions were practically the same for each condition, f_{0x}/f_{0y} ~0.99; it is thus possible to consider $f_{0x} = f_{0y} = f_0$. The damping coefficient in still water was inferior to ζ_w~5.5% in all the cases. The structural damping was low around $\zeta_s = 0.1\%$. The blockage effect coefficient was about 8.33% for all the tested conditions.

At least 35 velocity conditions were carried out for each configuration tested. The reduced velocity range performed was $2 < V_r < 15$, and the Reynolds number ($Re = UD/\upsilon$, where υ is the kinematic viscosity of the water) range was $3{,}000 < Re < 24{,}000$, which corresponds to current incidences of $0.02 < U < 0.22$m/s. Table 1 presents details about the conditions tested.

The Froude number ($Fr = U/\sqrt{gD}$) tested was lower than 0.2. As reported in Sakata *et al.* (2019), the free-end and the free-surface effects can be neglected for low aspect ratio cylinders for $Fr < 0.5$.

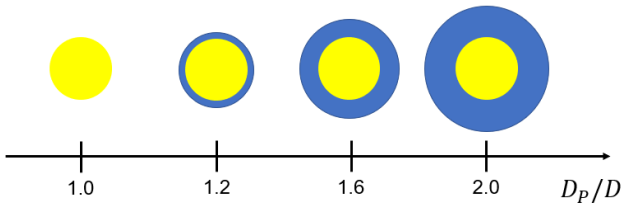

Fig 4. Illustration of the top view of the cylinders with different heave plate configurations.

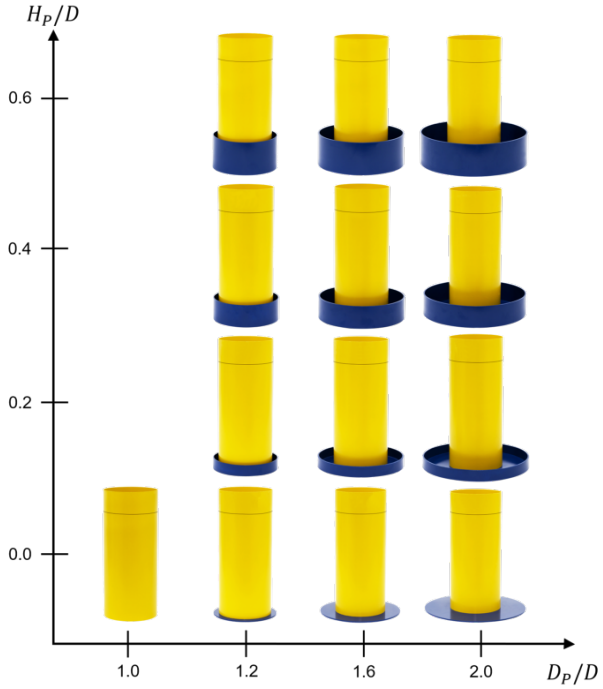

Fig 5. Illustration of the perspective view of the experimented cylinders with different heave plate configurations.

Table 1. Matrix of the conditions carried out.

$\frac{D_p}{D}$	$\frac{H_p}{D}$	T_0 [s]	ζ_w [%]	m [kg]	$C_a = m_a/m$	KG [m]
1.0	0.0	9.70	3.94	3.07	1.79	0.125
1.2	0.0	9.81	3.66	3.12	1.81	0.122
1.6	0.0	9.98	3.75	3.16	1.84	0.120
2.0	0.0	10.13	3.42	3.20	1.88	0.117
1.2	0.2	9.92	3.69	3.14	1.83	0.121
1.6	0.2	10.07	4.09	3.20	1.85	0.117
2.0	0.2	10.35	4.97	3.28	1.91	0.114
1.2	0.4	10.03	3.79	3.18	1.85	0.120
1.6	0.4	10.38	4.89	3.27	1.93	0.114
2.0	0.4	10.78	5.49	3.35	2.03	0.111
1.2	0.6	10.12	3.73	3.22	1.86	0.119
1.6	0.6	10.81	4.51	3.33	2.05	0.113
2.0	0.6	11.36	4.75	7.55	2.23	0.109

METHODOLOGY

The 6dof were measured during the tests. The VIM response was analyzed through the standard deviation (std) of displacements in the in-line and transverse directions. Moreover, as commonly found, dimensionless values, A_x/D, and A_y/D, were presented using the diameter of the column, D.

The reduced velocity $V_r = U/f_{0y}D$ was defined as a function of the incident current velocity, U, the natural frequency of the transverse motion in still water, f_{0y}, and the diameter of the column, D.

The mean drag force coefficient was calculated as:

$$C_D = 2\overline{FH_x}/(\rho S U^2)$$

where $\overline{FH_x}$ is the mean of the hydrodynamic force in the in-line direction, ρ is the water density, and S is the column area exposed to the current without the heave plate as $S = LD$.

RESULTS

The discussion of the results was divided into two groups to present the effect of the heave plate diameter and the heave plate height separately. All the results were compared with the fundamental case, i.e., the cylinder case without the heave plate.

The discussions were focused in the in-line and transverse directions, due to the low amplitudes observed in the other degrees of freedom (vertical and angular).

Fig 6 presents the non-dimensional amplitudes for the motions in the transverse direction, A_y/D, for the cases with the heave plate without height, i.e., $H_p/D = 0.0$. All the results revealed to be similar. The amplitudes for the motions in the transverse direction started to rise around $V_r = 3$ and reached the maximum value around $V_r = 10$. Reduced velocities larger than 10 could not be carried out for these cases due to the high values of the drag coefficient and the apparatus limitation. The maximum amplitudes in the transverse direction observed were approximately $A_y/D = 1.3$.

The presence of the heave plate height anticipated the rise of the amplitudes in the transverse direction. And the increase of the amplitudes was higher the larger the heave plate diameter was. Therefore, the effect was not meaningful.

The behavior started to change once the heave plates with height were included. For a constant value of heave plate height, as can be seen in Fig 7 to Fig 9, the increase of the heave plate diameter triggered a decrease in the amplitudes in the transverse direction and also a desynchronization of the VIM phenomenon with a significant drop of the amplitudes. This behavior could be a characteristic of the lower branch region.

The drop in the amplitudes of the motions in the transverse direction was related to the end of the synchronization range, i.e., the vortex shedding and the motions did not present the same frequency. The results of the PSD of the motions in the transverse direction, see Fig 27, showed that the start of the amplitude decrease was related to the loss of energy. The synchronization range started from $V_r = 5$ for all the cases and finished earlier the larger the heave plate diameter was for the same heave plate height. The frequency of the motions f_y/f_0noticeably had almost a linear behavior along with the reduced velocity; thus, the behavior presented a constant "Strouhal-like number," as commented by Gonçalves *et al.* (2018).

The high values of amplitude in the transverse direction,A_y/D, were due to the presence of more than one degree of freedom. The possibility of oscillation in the in-line direction and also synchronized with the transverse one promoting high amplitudes was reported by Jauvtis & Williamson (2004). The presence of the free-end effects due to the three-dimensional structures, e.g., the arch-type vortex, included another low-frequency structure that contributed to high amplitudes as discussed by Gonçalves *et al.* (2015, 2018). It is important to highlight that that the system had a small mass ratio due to the floating characteristic, i.e., $m^* = 1$; and, in this case, the high amplitudes can be found as explained by Jauvtis and Williamson (2004).

Fig 10 to Fig 13 present the non-dimensional amplitude results for the motions in the in-line direction, A_x/D, for the cases with the constant heave plate heights, $H_p/D = 0.0$, 0.2, 0.4, and 0.6, respectively. The behavior was the same as the one discussed for the motions in the transverse direction. The maximum value observed was $A_x/D = 0.5$, which was lower than the one presented for motions in the transverse direction.

The PSD results of the motions in the in-line direction, see Fig 28, showed reasonable energy in the synchronization range. However, the ratio of frequencies in the in-line direction,f_x/f_0, was twice the value of the one in the transverse direction,f_y/f_0, i.e., the frequency of the in-line motion was twice the frequency of the transverse motion; thus, $f_x/f_y = 2$. The double frequency of the in-line motion is a typical value encountered for systems with 2dof and small mass ratio, as discussed in Jauvtis & Williamsom (2004), Blevins & Coughran (2009), and Gonçalves *et al.* (2013).

The synchronization of the motions in the in-line and transverse direction characterized by the ratio $f_x/f_y = 2$ was responsible for the higher values of the mean drag in that range of reduced velocity in the synchronization range. Fig 14 to Fig 17 present the mean drag force coefficient, $\overline{C_x}$, for the cases with the constant heave plate heights, $H_p/D = 0.0$, 0.2, 0.4, and 0.6, respectively. All the values were presented using the projected area of the fundamental cylinder case, i.e., $S = LD$. The increase of the drag inside synchronization range is known as dynamic amplification of the drag, as reported by Blevins (1990) and Jauvtis & Williamson (2004).

For the cases without the heave plate height, the mean drag coefficient was higher than the cylinder without the heave plate, and the value for the largest heave plate diameter was the highest. The maximum amplitude was $\overline{C_x}$~5.5 for the case without the heave plate height and $\overline{C_x}$~4.0 for the cylinder without heave plates.

For the cases with heave plate height, the mean drag coefficient was lower than the column without heave plates. The increase of the heave plate diameter promoted a decrease in the drag force. In the high values of the reduced velocity, where the lower branch and no synchronization was observed, the mean drag coefficient was similar to the fixed cylinder case $\overline{C_x}$~1.0 as reported by Gonçalves *et al.* (2015).

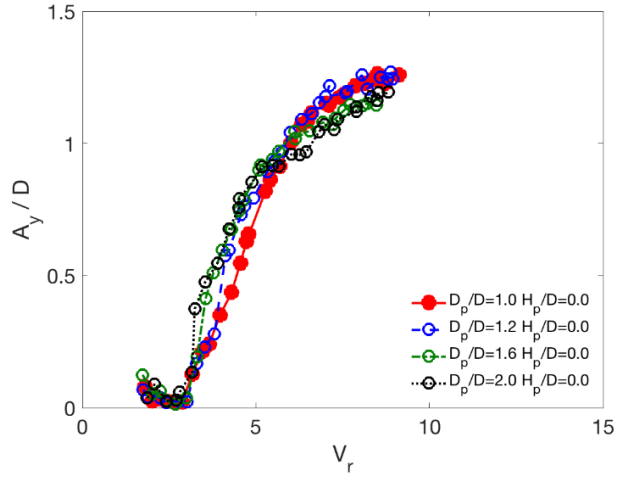

Fig 6. Non-dimensional amplitude for the motions in the transverse direction for $H_p/D = 0.0$ and different heave plate diameters.

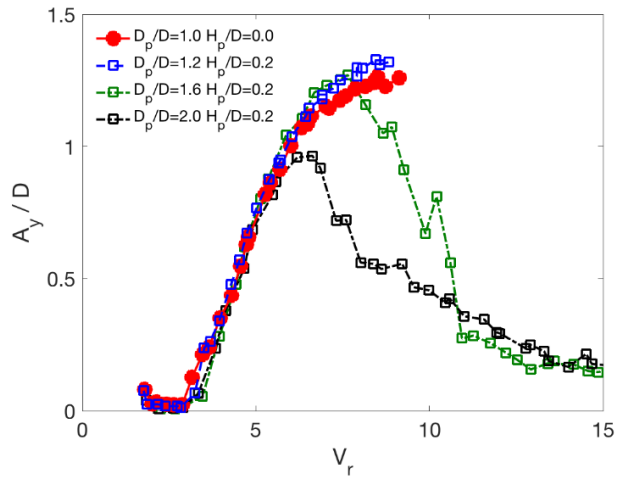

Fig 7. Non-dimensional amplitude for the motions in the transverse direction for $H_p/D = 0.2$ and different heave plate diameters.

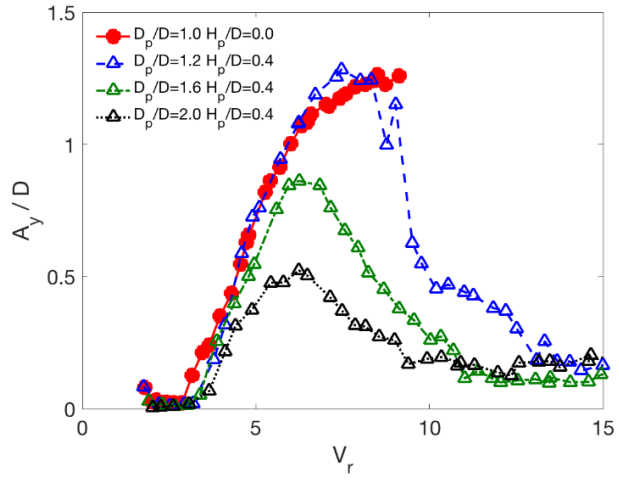

Fig 8. Non-dimensional amplitude for the motions in the transverse direction for $H_p/D = 0.4$ and different heave plate diameters.

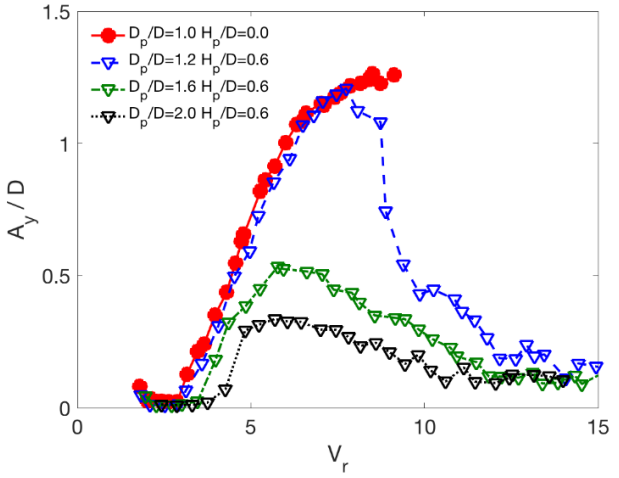

Fig 9. Non-dimensional amplitude for the motions in the transverse direction for $H_p/D = 0.6$ and different heave plate diameters.

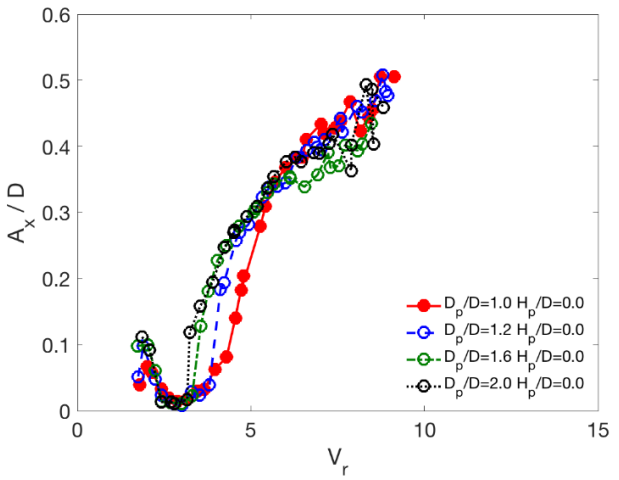

Fig 10. Non-dimensional amplitude for the motions in the in-line direction for $H_p/D = 0.0$ and different heave plate diameters.

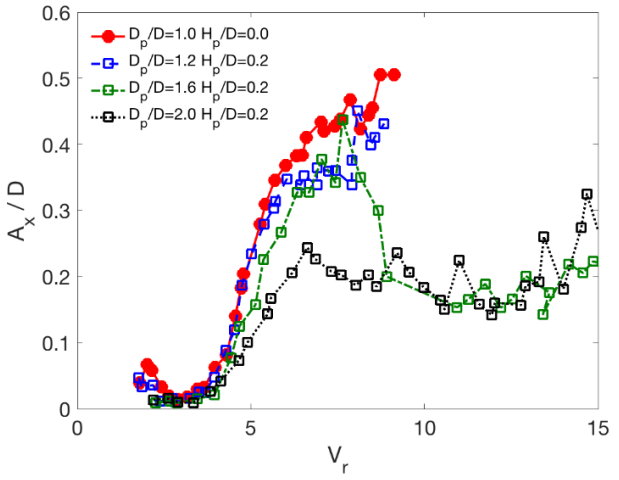

Fig 11. Non-dimensional amplitude for the motions in the in-line direction for $H_p/D = 0.2$ and different heave plate diameters

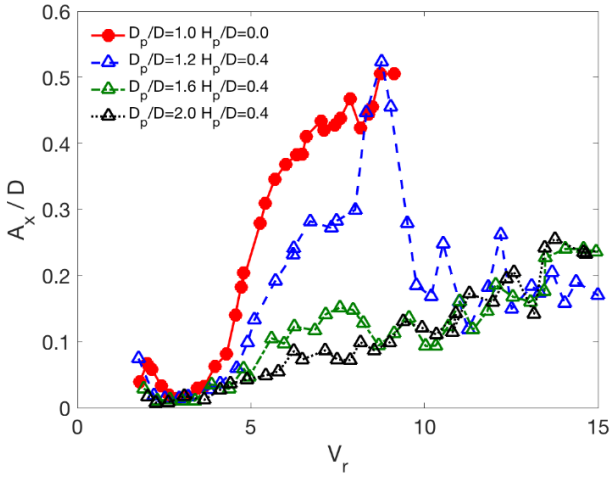

Fig 12. Non-dimensional amplitude for the motions in the in-line direction for $H_p/D = 0.4$ and different heave plate diameters.

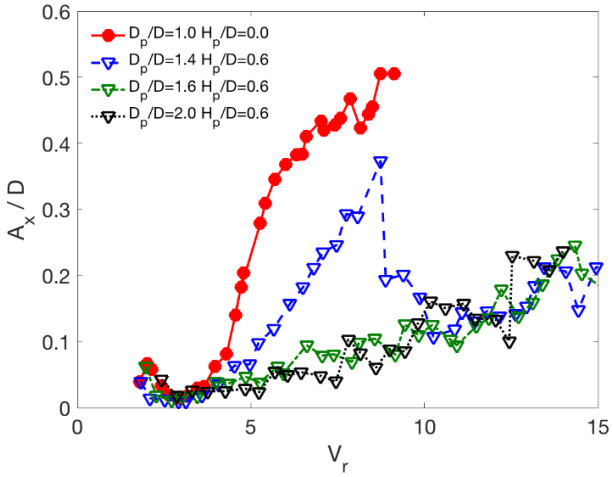

Fig 13. Non-dimensional amplitude for the motions in the in-line direction for $H_p/D = 0.6$ and different heave plate diameters.

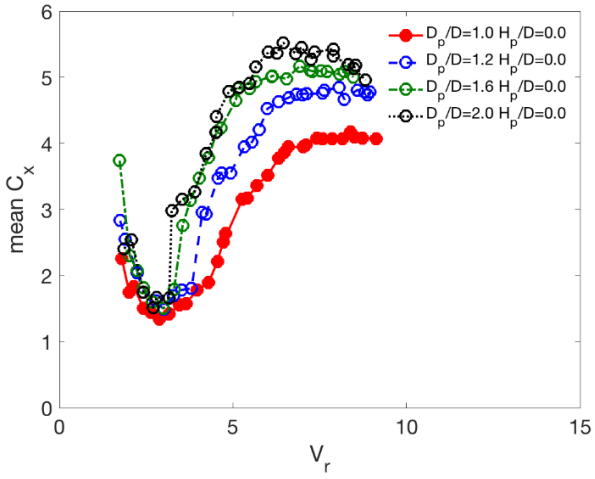

Fig 14. Mean drag force coefficient for $H_p/D = 0.0$ and different heave plate diameters.

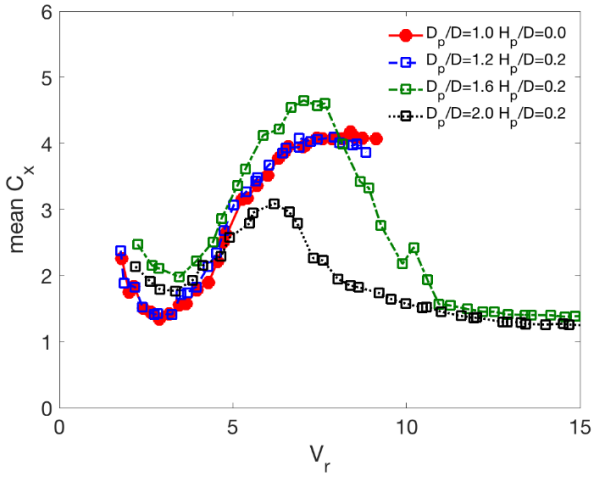

Fig 15. Mean drag force coefficient for $H_p/D = 0.2$ and different heave plate diameters.

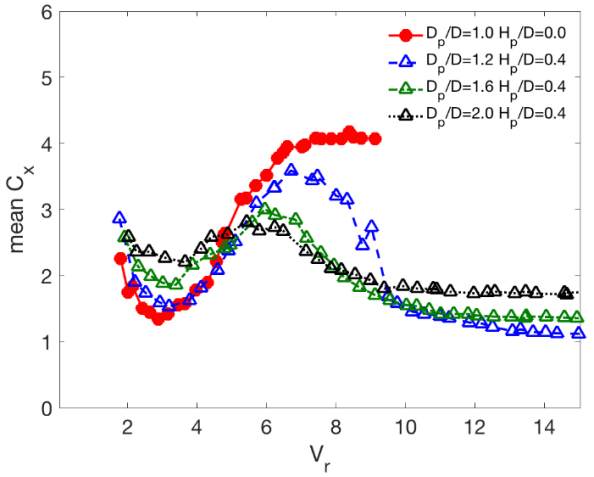

Fig 16. Mean drag force coefficient for $H_p/D = 0.4$ and different heave plate diameters.

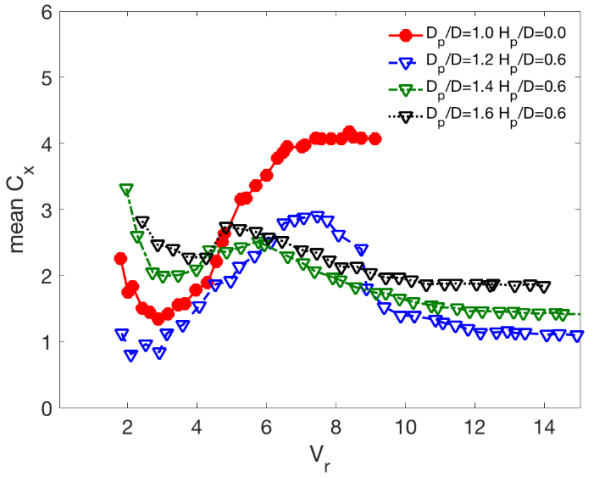

Fig 17. Mean drag force coefficient for $H_p/D = 0.6$ and different heave plate diameters.

Aiming to understand the heave plate height effect on the VIM, the results can be presented using a constant value of heave plate diameter and changing the heave plate height.

Fig 18 presents the non-dimensional amplitudes for the motions in the transverse direction, A_y/D, for the cases with different heave plate heights and a constant diameter, $D_p/D = 1.2$. All the results showed to be similar until the end of the synchronization. The amplitudes of the motions in the transverse direction started to rise around $V_r = 3$. The heave plate height affected the end of the synchronization. The end of the synchronization was earlier the larger the heave plate height was.

The same behavior can be observed for $D_p/D = 1.6$ and $D_p/D = 2.0$, as presented in Fig 19, and Fig 20, respectively. The effect of the heave plate height was more significant the larger the heave plate diameter was. The decrease of the amplitudes was substantial for the cases with $D_p/D = 2.0$ compared to the cylinder without a heave plate.

The same behavior can be observed for the motions in the in-line direction, as presented in Fig 21 to Fig 23, for D_p/D =1.2 to 2.0, respectively.

The presence of the heave plate height added a second characteristic diameter to the column span. The second diameter may be responsible for desynchronizing the vortex structures around the column. It can be possible to promote the early existence of the drop of the amplitudes or lower branch. The increase in the heave plate height caused a significant modification on the amplitude values in the transverse direction.

The new aspect ratio of the cylinder due to the presence of the heave plate could be calculated as $AR_p = (L - H_p)/D$. The behavior followed the results presented by Gonçalves *et al.* (2018), in which the results allowed concluding that the amplitudes in the transverse direction decreased with the decrease of the aspect ratio.

Fig 24 to Fig 26 present the mean drag coefficient, $\overline{C_x}$, for the cases with the constant heave plate diameter, D_p/D =1.2, 1.6, and 2.0, respectively. In general, the drag force coefficient decreased by increasing the heave plate height for a constant heave plate diameter, and the drag force coefficient for the case without heave plate height was higher than the one for the cylinder without the heave plate.

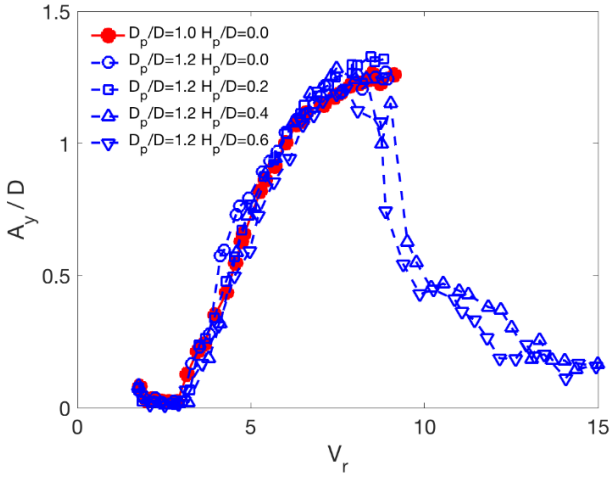

Fig 18. Non-dimensional amplitude for the motions in the transverse direction for $D_p/D = 1.2$ and different heave plate heights.

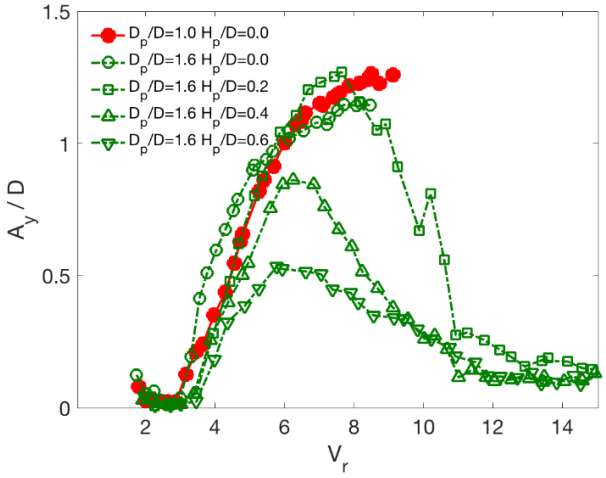

Fig 19. Non-dimensional amplitude for the motions in the transverse direction for $D_p/D = 1.6$ and different heave plate heights.

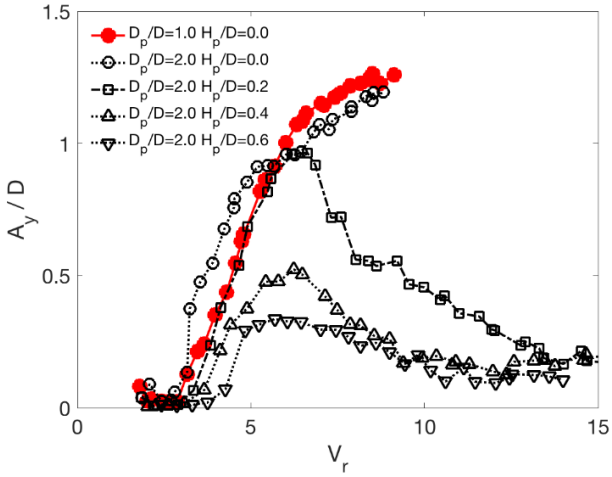

Fig 20. Non-dimensional amplitude for the motions in the transverse direction for $D_p/D = 2.0$ and different heave plate heights.

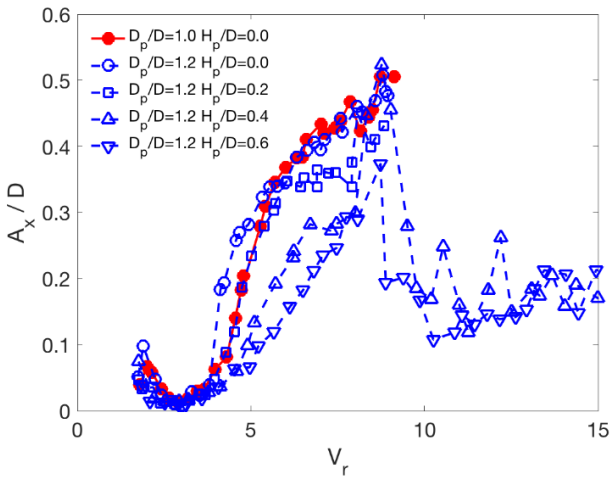

Fig 21. Non-dimensional amplitude for the motions in the in-line direction for $D_p/D = 1.2$ and different heave plate heights.

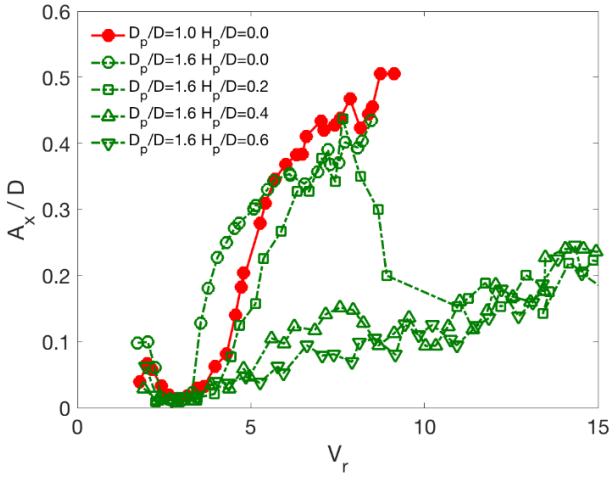

Fig 22. Non-dimensional amplitude for the motions in the in-line direction for $D_p/D = 1.6$ and different heave plate heights.

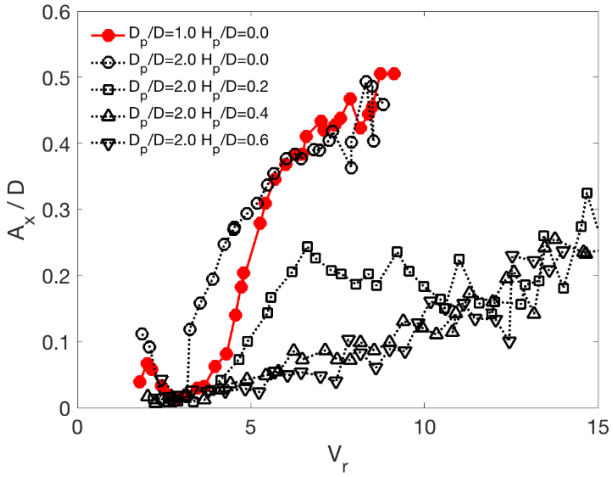

Fig 23. Non-dimensional amplitude for the motions in the in-line direction for $D_p/D = 2.0$ and different heave plate heights.

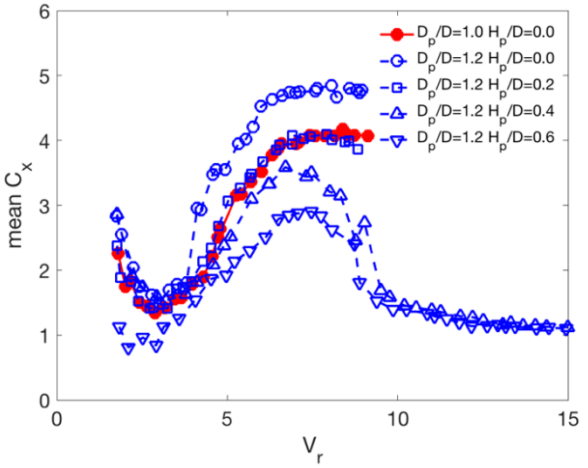

Fig 24. Mean drag force coefficient for $D_p/D = 1.2$ and different heave plate heights.

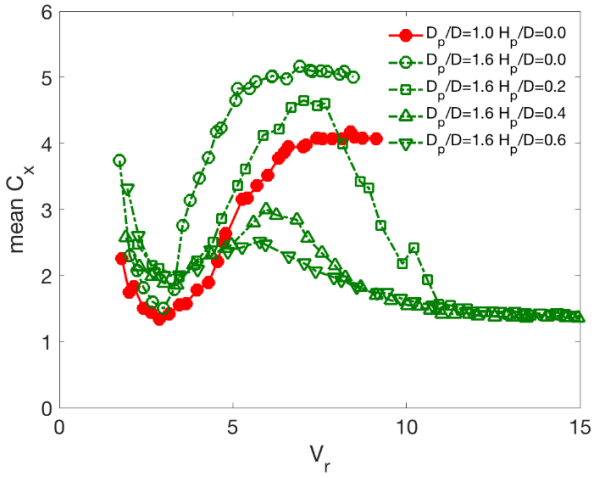

Fig 25. Mean drag force coefficient for $D_p/D = 1.6$ and different heave plate heights.

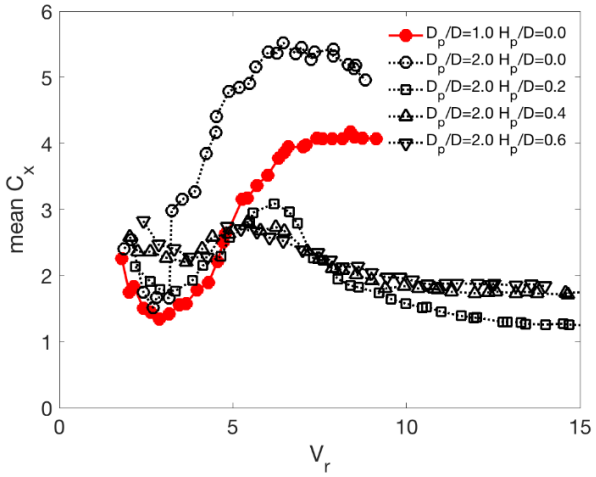

Fig 26. Mean drag force coefficient for $D_p/D = 2.0$ and different heave plate heights.

CONCLUSIONS

Experiments were carried out in a recirculating water channel regarding the VIM of floating single circular cylinders with heave plates. 6dof motions were recorded using an optical capture system. The model was supported elastically by four linear springs that kept similar stiffness in the in-line and transverse direction. The Reynolds number range was $3{,}000 < Re < 24{,}000$ that comprised a reduced velocity range of $2 < V_r < 15$.

The aim was to verify the effects of the heave plate dimensions, namely diameter, D_p, and height, H_p, on the VIM amplitudes. Results of amplitudes and PSD for the in-line and transverse directions, as well as the drag force coefficient, were evaluated.

In general, the increase in the heave plate dimensions decreased the VIM amplitudes. The presence of the heave plate was responsible for including the end of the synchronization range or lower branch behavior. The drop in the amplitudes could not be observed for the column without the heave plate and also for the cases with the heave plate without the heave plate height.

For the mean drag coefficients, the results with heave plate without heave plate height, $H_p/D = 0.0$, were higher than for the cylinder case without the heave plate, with the highest value, $\overline{C_x}$~5.5, for the largest heave plate height, $H_p/D = 1.6$. However, the drag results decreased with the increase of the heave plate height, and the same results were lower than the column without the heave plate.

The presence of the heave plate height was an excellent feature to decrease VIM amplitudes and also the drag force around a single cylinder. It may be a useful feature for mitigating amplitudes for single-column floater systems. Those findings can be used in the design of the platform systems from the flow structure interaction point of view. Studies to understand the effects of heave in waves were conducted to choose the best geometry of the heave plates and to obtain an optimized multi-column FOWT system, as in Mello *et al.* (2019). The VIM behavior of multi-column systems with heave plates must be investigated to understand if the conclusion herein can be extrapolated from the single to the multi-column cases.

ACKNOWLEDGEMENTS

This work was supported by The Japan Society of Naval Architects and Ocean Engineers (JASNAOE) throughout the project "Brazil-Japan Collaborative Research Program 2018/2019".

The authors would like to thank the JSPS (Japan Society for the Promotion of Science) for the opportunity and support given throughout the "Bilateral Joint Research Projects between Japan and Brazil".

The first author thanks the JSPS for the grant as a JSPS International Research Fellow (P18355, Graduate School of Engineering, The University of Tokyo), KAKENHI Grant Number JP18F18355, and also the Brazilian National Council for Scientific and Technological Development (CNPq) for grant 200096/2017-6.

REFERENCES

Assi, GRS, Meneghini, JR, Aranha, JAP, Bearman, PW, and Casaprima, E (2006) "Experimental investigation of flow-induced vibration interference between two circular cylinders," *Journal of fluids and structures*, 22, pp. 819-827.

Barrio, AB, Ruano, SF, Loureiro, AM, Fernandez, EM, Buron, FM, Escudero, JO, Tubio, JR, Gomez, CS, Peces, AV, Pavon, CL, and Iglesias, AS (2019) "Scale effects on heave plates forsemi-submersible floating offshore windturbines: case study with a solid plain plate," *Journal of Offshore Mechanics and Arctic Engineering*, JOMAE-19-1041, accepted manuscript.

Blevins, RD (1990) "Flow-induced vibration," Krieger, Malabar, FL, USA.

Blevins, RD,and Coughran, CS (2009) "Experimental investigation of vortex-induced vibration in one and two dimensions with variable mass, damping, and Reynolds number," *Journal of Fluids Engineering*, 131, pp. 101202-7.

Carlson, DW, and Sadeghi, YM (2017) "Vortex-induced vibration of spar platforms for floating offshore wind turbines," *Wind Energy*, Vol. 21, pp. 1169-1176.

Gonçalves, RT, Rosetti, GF, Franzini, GR, Meneghini, JR, and Fujarra, ALC (2013) "Two degrees-of-freedom vortex-induced vibration of circular cylinders with very low aspect ratio and small mass ratio," *Journal of Fluids and Structures*, 39, pp. 237-257.

Gonçalves, RT, Franzini, GR, Rosetti, GF., Meneghini, JR,and Fujarra, ALC (2015) "Flow around circular cylinders with very low aspect ratio," *Journal of Fluids and Structures*, 54, pp. 122-141.

Gonçalves, RT, Meneghini, JR, and Fujarra, ALC (2018) "Vortex-induced vibration of floating circular cylinders with very low aspect ratio," *Ocean Engineering*, 154, pp. 234-251.

Gonçalves, RT, Chame, MEF, Silva, LSP, Koop, A, Hirabayashi, S and Suzuki, H (2019) "Experimental study on flow-induced motions (FIM) of a floating offshore wind turbine semi-submersible type (OC4 phase II floater)," *Proc. of the ASME 2019 2nd International Offshore Wind Technical Conference*, IOWTC2019-7513, St. Julian's, Malta.

Jauvtis, N, and Williamson, CHK (2004) "The effect of two degrees of freedom on vortex-induced vibration at low mass and damping," *Journal of Fluid Mechanics*, 509, pp. 23-62.

Lemmer, F, Yu, W, and Cheng, PW (2018) "Iterative frequency-domain response of floating offshore wind turbines with parametric drag," *Journal of Marine Science and Engineering*, 6, 118.

Li, J, Liu, S, Zhao, M, Teng, B (2013) "Experimental investigation of the hydrodynamic characteristics of heave plates using forced oscillation," *Ocean Engineering*, 66, 82-91.

Liu, Y, Li, S, Yi, Q, and Chen, D (2016) "Developments in semi-submersible floating foundations supporting wind turbines: A comprehensive review," *Renewable and Sustainable Energy Review*, 60, pp. 433-449.

Mello, PC, Alberto, IF, Malta, EB, Franzini, GR, Silva, ROP, Simos, AN, Candido, MHO, Gonçalves, RT, Carmo, LHS, and Suzuki, H (2019) "Influence of heave plates on the dynamics of a floating offshore wind turbine in waves," *Proc of the Annual Autumn Conference 2019 of the Japan Society of Naval Architects and Ocean Engineers*, Himeji, Japan.

Moreno, J, Cameron, M, Thiagarajan, KP, and Mendoza, CAG (2015) "Hydrodynamic performance of heave plates on floating offshore wind turbine platforms," *Proc of the 25th International Ocean and Polar Engineering Conference*, Hawaii, USA.

Pavon, CL, and Iglesias, AS (2015) "Hydrodynamic coefficients and pressure loads on heave plates for semi-submersible floating offshore wind turbines: A comparative analysis using large scale models," *Renewable Energy*, 81, 864-881.

Robertson, A, Jonkman, J, Masciola, M, Goupee, A, Coulling, A, and Luan, C (2014) "Definition of the semisubmersible floating system for phase II of OC4," in *Technical Report No. NREL/TP-5000-60601*, National Renewable Energy Lab. (NREL).

Sakata, K, Hirabayashi, S, Yoshimura, Y, Suzuki, H, and Gonçalves, RT (2019) "Free-surface effects on hydrodynamic forces of half-submerged circular cylinders with low aspect ratio," in *Proc of the 25th ABCM International Congress of Mechanical Engineering*, COB-2019-2379, Uberlândia, MG, Brazil.

Suzuki, H, Xiong, J, Carmo, LHS, Vieira, DP, Mello, PC, Malta, EB, Simos, AN, Hirabayashi, S, and Gonçalves, RT (2019) "Elastic response of a light-weight floating support structure of FOWT with guywire supported tower," *Journal of Marine Science and Technology*, 24, pp. 1015-1028.

Tao, L, and Cai, S (2004) "Heave motion suppression of a Spar with a heave plate," *Ocean Engineering*, 31, pp. 669-692.

Thiagarajan, KP, Ran, AZ, Tao, L, Datta, I, and Halkyard, JE (2002) "Influence of heave plate geometry on the heave response of classics spars," *Proc of the ASME 2002 21th International Conference on Ocean, Offshore and Arctic Engineering*, OMAE 2019-28350, Oslo, Norway.

FIGURES

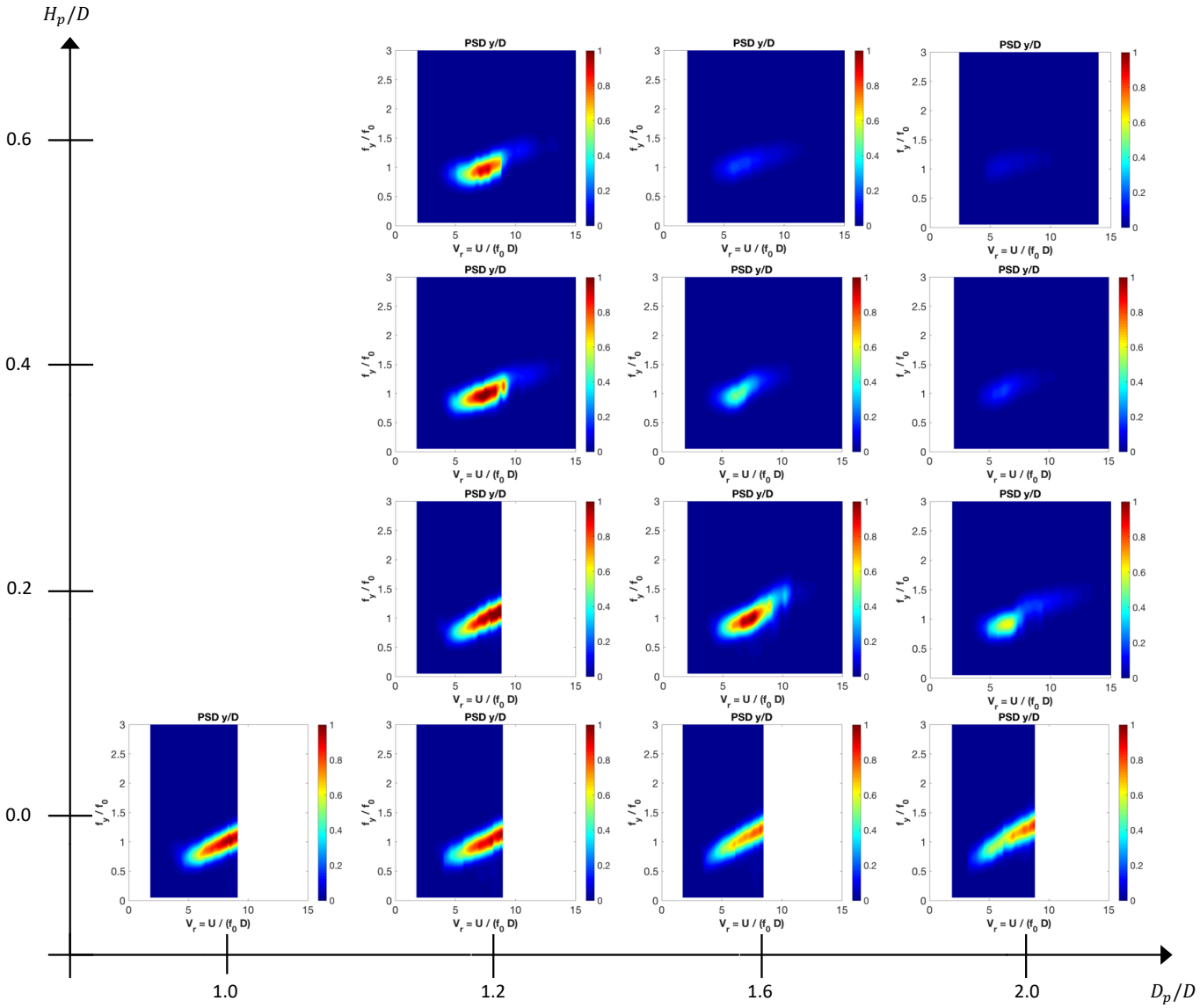

Fig 27. PSD of the motion in the transverse direction as a function of V_r for different values of heave plate diameter D_p/D (horizontal axes) and different values of heave plate heights H_p/D (vertical axes).

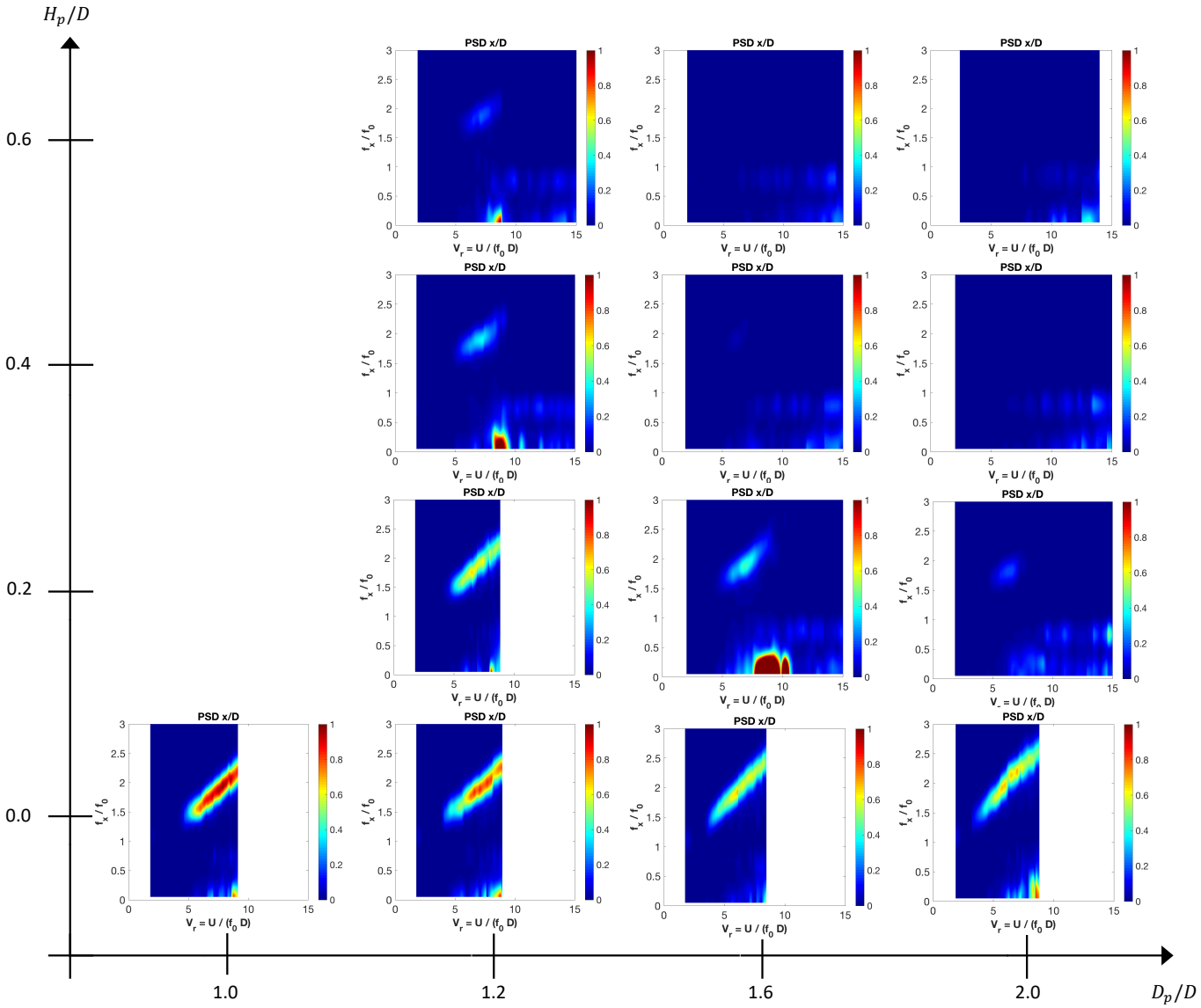

Fig 28. PSD of the motion in the in-line direction as a function of V_r for different values of heave plate diameter D_p/D (horizontal axes) and different values of heave plate heights H_p/D (vertical axes).